

## Numerical Simulation of Solid-liquid Flow in Hydrocyclone

J. Zhang, X.-Y. You, and Z.-G. Niu

School of Environmental Science and Engineering,  
Tianjin University, Tianjin 300072, China

Original scientific paper

Received: July 19, 2010

Accepted: February 16, 2011

Hydrocyclone is widely used as the centrifugal separation equipment to separate, classify and concentrate the product. In this paper, the multiphase flow models of mixture and Euler-Euler are used to simulate the internal three-dimensional flow field of hydrocyclone. It is found that compared to the experiment, the mixture model is shown to have the best performance among the models of mixture, Euler-Euler and discrete phase for the separation simulation when the diameter of solid particle is less than 30  $\mu\text{m}$ . Otherwise, the discrete phase model holds the best performance. Furthermore, the field of static pressure, axial and tangential velocity, and volume fraction in the hydrocyclone is obtained by the mixture model. The outcome is very helpful to explain the separation procedure and optimize the hydrocyclone design.

*Key words:*

Hydrocyclones, solid-liquid flow, separation, mixture model, Euler-Euler model

### Introduction

In the field of solid-liquid separation, hydrocyclone is widely used equipment for wet-mechanical separation such as slurry concentration, liquid clarification, solid-phase particles washing, liquid degassing and desanding, solid particle grading and classification, gas-liquid separation, two non-miscible liquids separation and so on. Hydrocyclone has simple structure consisting of feeding tube, underflow pipe, overflow tube, cylinder and cone. When the multiphase mixture to be separated enters into the hydrocyclone tangentially from upside under certain pressure, it results in a strong rotation. Due to the existence of density difference between the phases, most of the heavy phase discharges from the underflow opening, and most of the light phase discharges from the overflow port under the combined effects of centripetal buoyancy and fluid drag force.

Although the geometry structure of hydrocyclone is simple, the distribution of the internal flow field is extremely complex. Many approaches have been carried out and fruitful results have been achieved. With the development of computer, the internal flow field of hydrocyclone can be simulated by the method of computational fluid dynamics (CFD) which has great significance in elevating the design levels of cyclone, shortening design cycles, reducing development costs and improving operational efficiency.

Lu *et al.*<sup>1</sup> established a two-dimensional numerical model for the internal flow of hydrocyclone. Their results showed that the strongly swirling turbulent flow enclosed by Reynolds stress

model (RSM) agrees with the results of experiment better than that predicted by RNG (renormalization group)  $\kappa$ - $\epsilon$  model. Unfortunately, the internal flow of hydrocyclones cannot be truly modeled by a 2-D model due to the non-axisymmetric nature at the feed inlet opening. Zhao *et al.*<sup>2</sup> applied the stream function of continuous phase of Bloor and Ingham<sup>3</sup> to analyze the fluid particle trajectories, and a particle model of transportation ratio and separation efficiency was established. Schuetz *et al.*<sup>4</sup> concluded that the results of discrete phase simulation were better than those of the semi-empirical formula shown in their paper by comparing it to the experiment data. Narasimha *et al.*<sup>5</sup> investigated the separation efficiency of solid particles and the particle trajectories in the hydrocyclone. Gupta *et al.*<sup>6</sup> simulated air core and vortex in the hydrocyclone by volume of fluid (VOF) and RNG  $\kappa$ - $\epsilon$  for the enclosure of turbulence model. The formation mechanism of air core and vortex was discussed. Wang *et al.*<sup>7</sup> applied the Euler-Euler and Reynolds stress model to simulate the liquid-solid flow field, and they confirmed that the liquid-solid separation occurs mainly in the cone area. Recently, the turbulent flow of gas and liquid was modelled using Reynolds stress model, and the interface between the liquid and air core was modelled using the volume of fluid multiphase model. The results were then used in the simulation of particle flow described by the stochastic Lagrangian model.<sup>8–10</sup>

Currently, most approaches adopt Euler-Lagrangian model to simulate the liquid-solid flow in hydrocyclones. One key limitation of Euler-Lagrangian model is that the dispersed phase must occupy a low volume fraction (less than 10 %). Therefore,

the model is hard to apply in the simulation of liquid-solid flow in hydrocyclones since the flow is usually very dense, with the fraction of solid in the feed as high as 20 % under normal operating conditions. To overcome this problem, the mixture model and Euler-Euler model were used to simulate the multiphase flow of hydrocyclone. The feasibility and superiority of these models are demonstrated and the detailed results of mixture model are presented.

## Model description

### Mixture model

Mixture model is a simplified multiphase flow model. This model is generally used to simulate the flow where each phase has small speed difference and the coupling between the phases is strong. The model mainly solves the mixed-phase continuous and momentum equations written as

$$\frac{\partial \rho_m}{\partial t} + \nabla \cdot (\rho_m \vec{v}_m) = 0 \quad (1)$$

Where  $\rho_m$  and  $\vec{v}_m$  are density and velocity of the mixture. They are defined as

$$\rho_m = \sum_{k=1}^n \alpha_k \rho_k, \quad \vec{v}_m = \frac{\sum_{k=1}^n \alpha_k \rho_k \vec{v}_k}{\rho_m}$$

Where  $\rho_k$  is density of phase  $k$ ,  $n$  is the number of phase,  $\alpha_k$  is the volume fraction of phase  $k$  varying between 0 and 1,

The momentum equation is

$$\begin{aligned} & \frac{\partial}{\partial t} (\rho_m \vec{v}_m) + \nabla \cdot (\rho_m \vec{v}_m \vec{v}_m) = \\ & = -\nabla p + \nabla \cdot [\mu_m (\nabla \vec{v}_m + \nabla \vec{v}_m^T)] + \\ & + \rho_m \vec{g} + \vec{F} + \nabla \cdot \left( \sum_{k=1}^n \alpha_k \rho_k \vec{v}_{dr,k} \vec{v}_{dr,k} \right) \end{aligned} \quad (2)$$

Where  $p$  is the pressure,  $\vec{F}$  is the volume force and  $\mu_m$  is the viscosity of the mixture

$$\mu_m = \sum_{k=1}^n \alpha_k \mu_k$$

$\vec{v}_{dr,k}$  is the drift velocity of the secondary phase  $k$

$$\vec{v}_{dr,k} = \vec{v}_k - \vec{v}_m$$

### Euler-Euler model

Euler-Euler model governs the velocity and pressure of each phase and the interface between phases are coupled by the exchange coefficients. Each phase independently satisfies the law of conservation of mass and momentum. The continuity equation for phase  $k$  as

$$\frac{\partial}{\partial t} (\alpha_k \rho_k) + \nabla \cdot (\alpha_k \rho_k \vec{v}_k) = 0 \quad (3)$$

The momentum balance for phase  $k$  yields

$$\begin{aligned} & \frac{\partial}{\partial t} (\alpha_k \rho_k \vec{v}_k) + \nabla \cdot (\alpha_k \rho_k \vec{v}_k \vec{v}_k) = \\ & = -\alpha_k \nabla p + \nabla \cdot \bar{\bar{\tau}}_k + \sum_{p=1}^n \vec{R}_{qk} + \\ & + \alpha_k \rho_k \vec{g} + (\vec{F}_k + \vec{F}_{\text{lift},k} + \vec{F}_{\text{vm},k}) \end{aligned} \quad (4)$$

Where  $\bar{\bar{\tau}}_k$  is the stress-strain tensor of phase  $k$

$$\bar{\bar{\tau}}_k = \alpha_k \mu_k (\nabla \vec{v}_k + \nabla \vec{v}_k^T) + \alpha_k \left( \lambda_k - \frac{2}{3} \mu_k \right) \nabla \cdot \vec{v}_k \bar{\bar{I}}.$$

$\alpha_k$ ,  $\rho_k$  and  $\vec{v}_k$  is the volume fraction, density and velocity of phase  $k$ , respectively.  $\vec{F}_k$  is the external volume force,  $\vec{F}_{\text{lift},k}$  is a lift force,  $\vec{F}_{\text{vm},k}$  is virtual mass force,  $\vec{R}_{qk}$  is interaction force between the phases,  $p$  is the pressure shared by all phase,  $\bar{\bar{I}}$  is the unit tensor.

## Results and discussion

### Simulation conditions

Our approach is compared with the experiment of Bhaskar *et al.*<sup>11</sup> Fig. 1 shows the geometry of hydrocyclone. The detail of geometry parameters is described in Table 1.

Table 1 – Dimension details of hydrocyclone (mm)

CD	CyL	VFD	VFL	FI (l × w)	CA*	SPD
76	85	25	90	20 × 10	10°	10

CD, cyclone diameter; CyL, cylindrical length; VFD, vortex finder diameter; VFL, vortex finder length; FI, feed inlet dimensions (length × width); CA\*, cone angle in degrees; SPD, spigot diameter.

The equations of Mixture model and Euler-Euler model are solved by commercial Fluent software. Flow simulation is carried out using a 3-D double precision, steady state, and segregated solver. For turbulence calculations,  $k - \varepsilon$  RNG turbulence model is adopted.

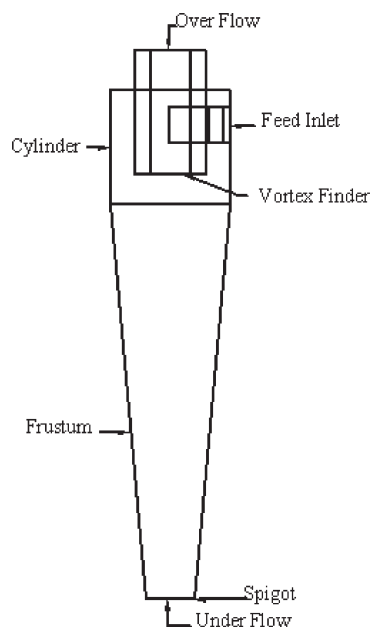


Fig. 1 – Geometry of hydrocyclone

After careful grid check, the computational domain is divided by 147073 cells of unstructured tetrahedral grids. The primary phase is water with the density of  $998.2 \text{ kg m}^{-3}$  and the second phase is solid particles with a density of  $2300 \text{ kg m}^{-3}$ . The mass fraction of solid phase is 10 % at the inlet. The diameter of particle ranges from  $1 \mu\text{m}$  to  $40 \mu\text{m}$ . The RSM model, which has been proven an appropriate turbulence model for cyclone flow, is adopted.<sup>12</sup> The continuity residual convergence criterion is  $10^{-6}$ . For a fast numerical convergence, the boundary conditions of constant gauge pressure at input and two outputs are used. The pressure at inlet and outlet is fixed as  $83 \text{ kPa}$  and  $0 \text{ kPa}$ , respectively. For this pressure input, the corresponding feed mass rate at inlet is  $1.23 \text{ kg s}^{-1}$  for mixture model and  $1.3 \text{ kg s}^{-1}$  for mixture model, which is much closer to  $1.16 \text{ kg s}^{-1}$  of experiment.<sup>11</sup>

### Model validation

Mixture model and Euler-Euler model of multiphase flow are chosen here. Fig. 2 shows the results of mixture model and Euler-Euler model compared with the results of experiment and the discrete phase model of Bhaskar *et al.*<sup>11</sup> Although the results of three models, i.e. the mixture model, the Euler-Euler model and the discrete phase model agree well with the experimental data, the performance of different models in different particle diameter range shows different behavior. The performance of mixture model and Euler-Euler model is better than that of discrete phase model when the diameter of particle is less than  $25 \mu\text{m}$  because the small particles couples with water phase and the ve-

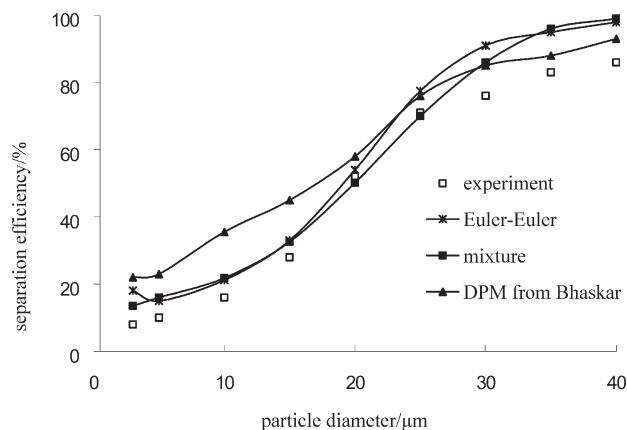


Fig. 2 – Separation efficiency of experiment and models

locity between the two phases is small. This is very favorable to the application of mixture model and Euler-Euler model. The discrete phase model gives better results for the larger particle diameter case, where the velocity between the two phases is large and the direct particle tracing is needed. In addition, the mixture model has a better performance compared to Euler-Euler model when the diameter of particle is between  $2 \mu\text{m}$  and  $30 \mu\text{m}$ . The mixture model costs about 90 % computation time of Euler-Euler model. Therefore, the mixture model is selected in the following flow field study. The diameter of particle is chosen to be  $d_{50} = 20 \mu\text{m}$ , which is corresponding to the case of separation efficiency of 50 %. The experiment  $d_{50}$  is about  $19.4 \mu\text{m}$ .

### Exploration of air core

The strong rotational flow of liquid in a hydrocyclone creates a low-pressure axial core and a free liquid surface. Such a low-pressure core in a hydrocyclone may communicate directly with the atmosphere at outlets open to air. The air is inhaled through the apex and forms an air core, which often results in poor separation performance of hydrocyclone. For choosing the numerical model and possible reduction of computer simulation time, it is important to determine if the air core exists in the internal flow field of hydrocyclone.

For checking if the air core exists in the present hydrocyclone under the current operating conditions, the interface between the liquid and air core is tracked by the volume of fluid method.<sup>13</sup> Numerical results indicate that there is a small air core in the upper outlet of internal flow field under present operating conditions. Therefore, the effects of air core on the separation performance of hydrocyclone are assumed to be neglected in this approach. The assumption is proven suitable because our numerical results agree well with the experimental results.<sup>11</sup> For this reason, the volume of fluid method is not adopted in the following study.

## Pressure and flow field of hydrocyclone

The cylindrical coordinate system is chosen, where the origin of the coordinate is located at the geometric center of cylindrical upper surface of cyclone. In order to view the simulation results intuitively, 5 vertical z-axis cross-sections (i.e.  $z = -125$  mm,  $z = -200$  mm,  $z = -275$  mm,  $z = -350$  mm,  $z = -425$  mm) are chosen to view the distribution of pressure, velocity and volume fraction of the internal flow.

### Static pressure

Figs. 3 and 4 show the distribution of static pressure. It is found that the distribution of static pressure has certain symmetry with respect to z axis. The maximum static pressure at the different z-planes appears in the vicinity of the wall. From top to bottom, the maximum static pressure decreases. This characteristic static pressure makes the fluid near the wall flow down towards the underflow. The minimum static pressure at the different z-planes appears in the vicinity of axes and it increases from top to bottom. This characteristic minimum static pressure makes the fluid in the cyclone cone near the cylindrical axis flow towards the overflow.

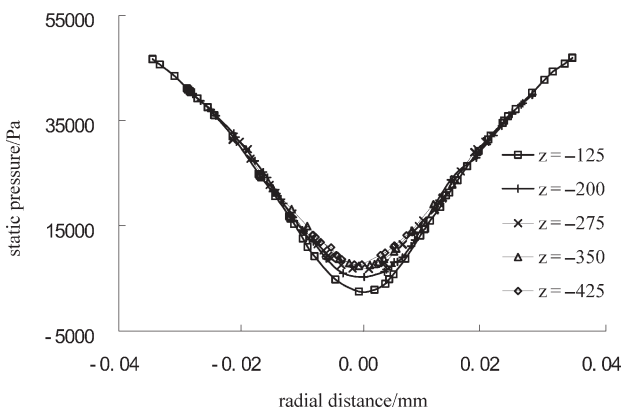


Fig. 3 – The static pressure along the radial axis  $\theta = 0$  at different height

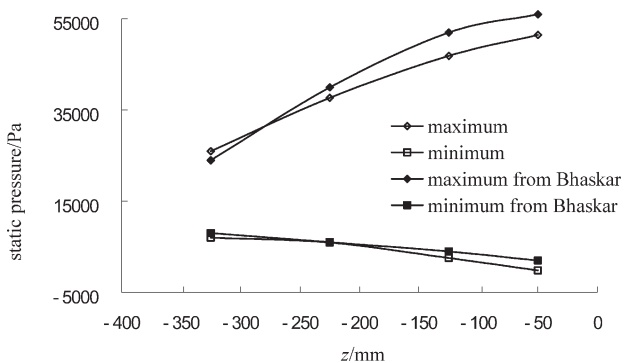


Fig. 4 – Maximum and minimum values of static pressures at different height

### Tangential velocity

The tangential velocity plays important roles in the performance of hydrocyclone because it is generally greater than the axial velocity and generates the centrifugal force for the separation of phases. Fig. 5 shows that the tangential velocity increases suddenly from the periphery to its maximum and decreases to the minimum in the vicinity of cylindrical axis.

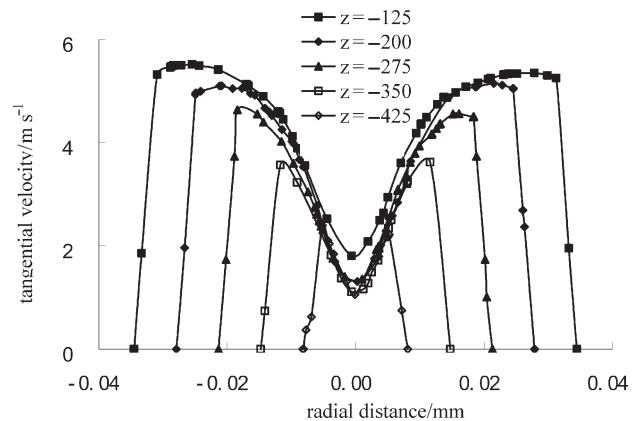


Fig. 5 – The tangential velocity along the radial axis  $\theta = 0$  at different height

### Axial velocity

Fig. 6 shows the axial velocity field. It is found that the fluid near the wall of hydrocyclone flows towards the underflow outlet and the fluid in the vicinity of cylindrical axis flows towards the overflow outlet. The axial velocity in the main cyclone separation zone decreases with the increase of the radial coordinate, and goes to zero at about 2/3 radius, then the velocity changes to negative with the increase of radius and reduces to zero at the hydrocyclone wall.

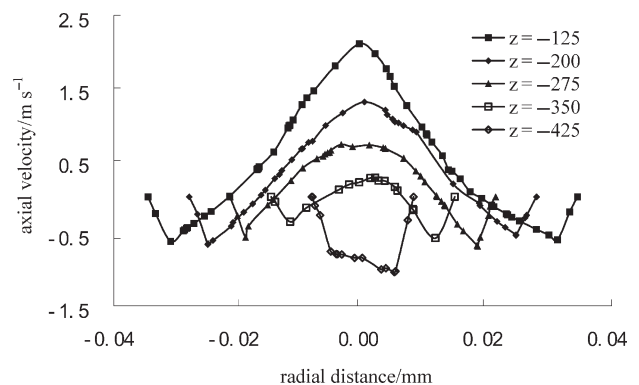


Fig. 6 – The axial velocity along the radial line  $\theta = 0$  at different height

### Volume fraction

Fig. 7 shows the volume fraction of water phase in hydrocyclone. It is found that the volume fraction of water increases from the wall to axis reaching the maximum in the vicinity of the vertical axis. It clearly shows the gradual accumulation of solid particles near the wall. The maximum volume fraction of water decreases as the  $z$  coordinate is reduced. The change of water volume fraction indicates clearly the process of particle and water separation in the hydrocyclone.

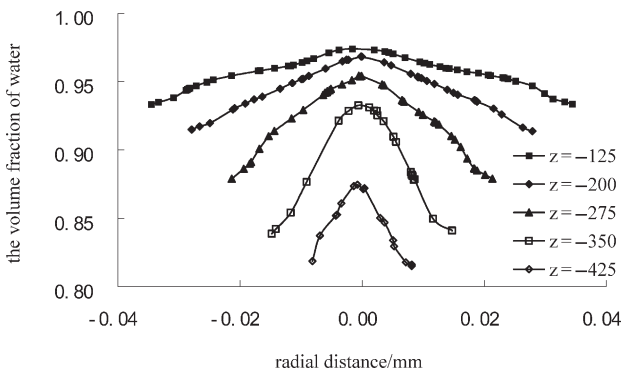


Fig. 7 – The volume fraction along the radial line  $\theta = 0$  at different height

### Conclusions

The three-dimensional mixture and Euler-Euler multiphase flow models are used to simulate the internal flow field of hydrocyclone by applying the RSM to enclose the turbulence stresses. The investigation leads to the following conclusions:

(1) The air core can be tracked by the volume of fluid method. Numerical results indicate that there is no air core in the internal flow field at present operating conditions;

(2) Compared with the experiments, it is found that the mixture model, the Euler-Euler model and the discrete phase model agree well with the experimental data. The mixture model shows a better performance than the Euler-Euler model and the discrete phase model for the solid-liquid separation simulation in the tested hydrocyclone when the diameter of solid particle is less than  $30 \mu\text{m}$ . Otherwise, the discrete phase model plays the best performance;

(3) The distribution of the static pressure, tangential and axial velocity, and water volume fraction in the hydrocyclone is obtained. The characteristic distribution of the above variable is very helpful to explain the separation procedure and optimize the hydrocyclone design.

### ACKNOWLEDGMENTS

The authors are grateful for the support of the Ministry of Science and Technology of China (2009BAC60B03) and National Natural Science Foundation of China (51008207).

### Nomenclature

- $d_{50}$  – particle diameter corresponding to 50 % separation efficiency
- $\vec{F}$  – volume force
- $\vec{F}_{\text{lift}}$  – lift force
- $\vec{F}_{\text{vm}}$  – virtual mass force
- $\vec{g}$  – gravity constant
- $\vec{I}$  – unit tensor
- $n$  – number of phase
- $p$  – pressure
- $r, \theta, z$  – cylindrical coordinate
- $\vec{R}$  – interaction force between the phases
- $t$  – time
- $\vec{v}$  – velocity vector

### Greek symbols

- $\alpha$  – volume fraction of phase
- $\rho$  – density
- $\mu$  – viscosity

### Subscripts

- $dr$  – drift velocity
- $k$  – phase index
- $m$  – value of mixture

### References

1. Lu, Y. J., Zhou, L. X., Shen, X., *Sci. China Ser. E.* **30** (2000) 47.
2. Zhao, Q. G., Xue, D. S., *J. Petroleum Univ., China*, **24** (2004) 62.
3. Bloor, M. I., Inghem, G. D. B., *J. Fluid Mech.* **178** (1987) 507.
4. Schuetz, S., Mayer, G., Bierdel, M., Piesche, M., *Int. J. Miner. Process.* **73** (2004) 229.
5. Narasimha, M., Sripriya, R., Banerjee, P. K., *Miner. Process.* **75** (2005) 53.
6. Gupta, R., Kaulaskar, M. D., Kumar, V., Sripriya, R., Meikap, B. C., Chakraborty, S., *Chem. Eng. J.* **144** (2008) 153.
7. Wang, L. Y., Zheng, Z. C., Wu, Y. X., Guo, J., Zhang, J., Tang, C., *J. Hydrodyn. Ser. B* **21** (2009) 408.
8. Wang, B., Yu, A. B., *Chem. Eng.* **135** (1–2) (2008) 33.
9. Ahmed, M. M., Ibrahim, G. A., Farghaly, M. G., *Miner. Process.* **91** (2009) 34.
10. Chu, K. W., Wang, B., Yu, A. B., Vince, A., Barnett, G. D., Barnett, P. J., *Miner. Eng.* **22** (2009) 893.
11. Bhaskar, K. U., Murthy, Y. R., Ramakrishnan, N., Srivastava, J. K., Sarkar, S., Kumar, V., *Miner. Eng.* **20** (2007) 290.
12. Bhaskar, K. U., Murthy, Y. R., Raju, M. R., Tiwari, S., Srivastava, J. K., Ramakrishnan, N., *Miner. Eng.* **20** (2007) 60.
13. You, X., Liu, W., Xiao, H., *Front. Archit. Civil Eng. in China* **3** (2009) 312.

